www.MaterialsViews.com

ADVANCED
ENERGY
MATERIALS
www.advenergymat.de

COMMUNICATION

SEI Growth and Depth Profiling on ZFO Electrodes by Soft X-Ray Absorption Spectroscopy

Andrea Di Cicco,* Angelo Giglia, Roberto Gunnella, Stephan L. Koch, Franziska Mueller, Francesco Nobili, Marta Pasqualini, Stefano Passerini, Roberto Tossici, and Agnieszka Witkowska

ZnFe$_2$O$_4$Li-ion batteries (LIBs) represent a reliable, affordable, and safe energy storage technology for use in portable application. However, current LIB active materials (graphite, lithium/transition metal spinel or layered oxides, olivine structures) can store only limited energy since they rely on insertion storage based on solid-state host-guest interactions. Moreover, performances and durability of the cells are strongly influenced by the characteristics of the solid electrolyte interphase (SEI),[1–3] which is formed upon the electrodes, especially for graphite, during the first charge/discharge cycle. This process is difficult to study and control. Recently, research efforts have been thus devoted both in devising new active materials (see for example refs.[4,5]) and in more accurate investigations of the SEI evolution mechanisms (see for example[6]). In particular, alternative charge/discharge mechanisms have been explored with the aim to reach higher energy densities using raw materials with lower costs and environmental impact. In this context, zinc iron oxide (ZnFe$_2$O$_4$, ZFO), encapsulated by a carbonaceous matrix (ZFO-C) has been recently developed[7–9] as an innovative anode material. This system has been found to be able to exchange Li$^+$ and e$^-$ both by conversion and alloying processes. As a consequence Fe, LiZn, Li$_2$O are formed upon lithiation, which are finely dispersed into a carbonaceous matrix,[7] according to a reversible reaction involving nine lithium ions per formula unit of ZFO and resulting in a capacity of ≈1000 mAh g^{-1}.[7] While the lithiation kinetics have already been probed by electrochemical impedance spectroscopy (EIS) and X-ray diffraction (XRD) analysis,[5,7] very little is known about the evolution of passivation layer properties on ZFO-C.

The aim of this work is to study the evolution of the SEI in this innovative anode material at selected charging steps by exploiting the surface sensitivity[10–12] of the soft X-ray absorption spectroscopy (XAS). This technique requires synchrotron radiation and was never used before for such a purpose, although it appears to be very suitable for a detailed depth profiling of the SEI of advanced electrodes. In fact, XAS experiments in the 50–1000 eV photon energy range can be typically performed using both total electron (TEY) and total fluorescence (TFY) yield techniques for which effective probing depths are around 2–10 nm and 70–200 nm, respectively. In this study, ex situ TEY and TFY X-ray absorption experiments have been conceived and realized to study the modification of the signals related to the various atomic species in ZFO-C electrodes selected at different states of charge during the first Li insertion process. XAS measurements have been preceded and corroborated by a complete electrochemical characterization including galvanostatic intermittent titration technique (GITT) and EIS, with the aim of correlating each XAS experiment with half-cell open-circuit potential (OCV) and charge, and to crosscheck the SEI evolution with the polarization of the electrodes.

The samples for the experiments were prepared using carbon-coated ZFO nanoparticles (ZFO-C), obtained[7] by dispersing 1 g of ZFO powder (<100 nm, Aldrich Chemistry) in 1.5 mL of an aqueous carbon precursor solution of sucrose (Acros Organics), followed by an annealing step under inert gas atmosphere. The weight ratio was 1:0.75 for ZFO:Suc. The obtained dispersion was homogenized by means of a planetary ball mill (Vario-Planetary Mill Pulverisette 4, FRITSCH, 2× 45 min at 400/–800 rpm with 10 min rest in between). Subsequently, the dispersion was dried at 70 °C under ambient atmosphere. After grinding, the resulting composite powder was annealed in a tubular furnace (R50/250/12, Nabertherm) at 450 °C for 4 h under a constant argon gas stream. The heating rate was set to 3 °C min^{-1}. The material was investigated by SEM (Scanning Electron Microscopy) and TEM (Transmission Electron Microscopy) revealing that it is formed by nanoparticles of average linear dimensions of about 50 nm, with formation of some

Prof. A. Di Cicco, Prof. R. Gunnella
Physics Division
School of Science and Technology
University of Camerino
62032 Camerino, MC, Italy
E-mail: andrea.dicicco@unicam.it
Dr. A. Giglia
CNR
Istituto Officina Materiali
34149 Trieste, Italy
S. L. Koch, F. Mueller, Prof. S. Passerini
Helmholtz Institute Ulm (HIU)
Helmholtzstr. 11, 89081 Ulm, Germany
S. L. Koch, F. Mueller, Prof. S. Passerini
Karlsruhe Institute of Technology (KIT)
P.O. Box 3640, 76021 Karlsruhe, Germany
Dr. F. Nobili, M. Pasqualini, R. Tossici
Chemistry Division
School of Science and Technology
University of Camerino
62032 Camerino, MC, Italy
Dr. A. Witkowska
Department of Solid State Physics
Gdansk University of Technology
Gabriela Narutowicza 11/12, 80-233 Gdańsk, Poland

COMMUNICATION

larger aggregates. XRD characterization revealed presence of nanocrystalline ZFO, while the lack of reflections related to graphitic carbon confirmed the amorphous nature of C-coating.

Composite electrodes were prepared by using Na-carboxymethylcellulose (CMC, Sigma-Aldrich) binder dissolved in deionized water (5:95 wt/wt). ZFO and SuperP carbon (MMM-Carbon), previously mixed and ground in an agate mortar were added to the binder solution resulting in a slurry with a ZFO:SuperP:CMC composition equal to 75:20:5 (mass ratio). After stirring overnight, the slurry was spread onto copper foil using the "Doctor Blade" technique and dried at 70 °C in air. 9 mm diameter circular electrodes, resulting in active material loadings of the order of 1–1.5 mg cm^{-2}, were cut and pressed applying a specific pressure of 11 tons cm^{-2}. Electrochemical three-electrode T-cells (Swagelock type) were assembled for samples conditioning, by using one ZFO-C electrode as working electrode and metal Li disks as counter and reference electrodes. LiPF$_6$ 1 M in EC:DMC 1:1 v:v (Solvionic) was used as electrolyte, and Whatmann GF/D as separator.

GITT was performed, as a series of galvanostatic steps (10 min each, at 50 mA g^{-1}), followed by open-circuit relaxation periods (60 min each), and then by EIS measurements at each of the obtained states of charge. The impedance measurements have been performed around equilibrium potential, superimposing a sinusoidal potential oscillation (amplitude ± 5 mV), in the frequency range 100 kHz to 1 Hz in order to investigate the evolution of interfacial polarizations. All potentials are given versus Li$^+$/Li couple. **Figure 1** reports the equilibrium capacity (Q) versus OCV (E) profile as acquired by GITT. The profile is consistent with previous findings[7] and describes the Li uptake by ZFO active material, leading to LiZn, Fe, Li$_2$O as final products of the mixed conversion/alloying processes, superimposed

Figure 2. Electrochemical impedance spectroscopy (EIS) response of a typical ZFO-C electrode at given potentials (see text) during the first Li uptake. The EIS response in an enlarged impedance range is shown in the inset.

to the irreversible Li storage by the carbonaceous matrix, which leads to the formation of the SEI upon electrode surface. The discharge capacity is about 1200 mAh g^{-1}, which allows to estimate about 20% first-cycle capacity loss for irreversible processes with respect to the nominal reversible capacity (1000 mAh g^{-1}).

Specific points in Figure 1, marked as (A), (B), (C), (D), correspond to capacity and potential values of the electrodes that later underwent ex situ XAS characterization. Point (A) corresponds to the fresh electrode. Lithiation of ZFO follows the increase of the capacity. Point (B) obtained at E = 1.02 V and Q = 83 mAh g^{-1} is related to the beginning of Li uptake by ZFO and limited SEI formation is expected. Points (C) and (D), obtained respectively at E = 0.87 V, Q = 167 mAh g^{-1} and at E = 0.79 V, Q = 417 mAh g^{-1}, correspond to the beginning and ending of a plateau in a potential region where most of SEI formation commonly occurs (see for example[3] and refs. therein).

Electrochemical impedance spectroscopy (EIS) was applied to the ZFO-C electrodes. **Figure 2** shows the evolution of the Nyquist plots of the ZFO-C electrode at given potential values. As Li content is increased and potential decreased, Li uptake kinetics are improved and the electrode impedance is greatly reduced (see inset), resulting in a contraction of the low-frequency arc. The inspection of the high-frequency region allows us to gain information about the evolution of SEI. The increase of the diameter of the high-frequency arc reveals the progressive growth of the passivation layer. However, most of this variation occurs from OCV to 0.79 V, which corresponds to points (A) and (D), respectively (see Figure 2). On the other hand, only minor changes are found for lower potentials, i.e., higher Li contents.

This trend confirms the electrochemical behavior of ZFO-C, detailed in refs.[7,13], showing that the irreversible capacity loss takes place completely during the first Li uptake, with a first-cycle coulombic efficiency of about 75%, while all the
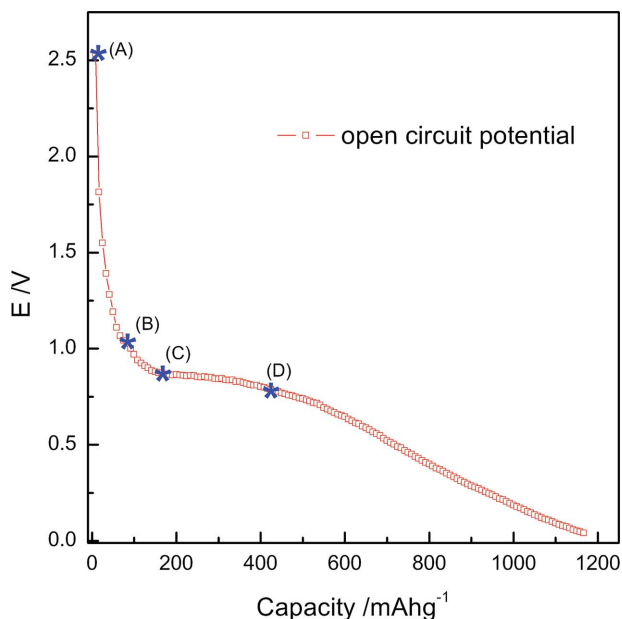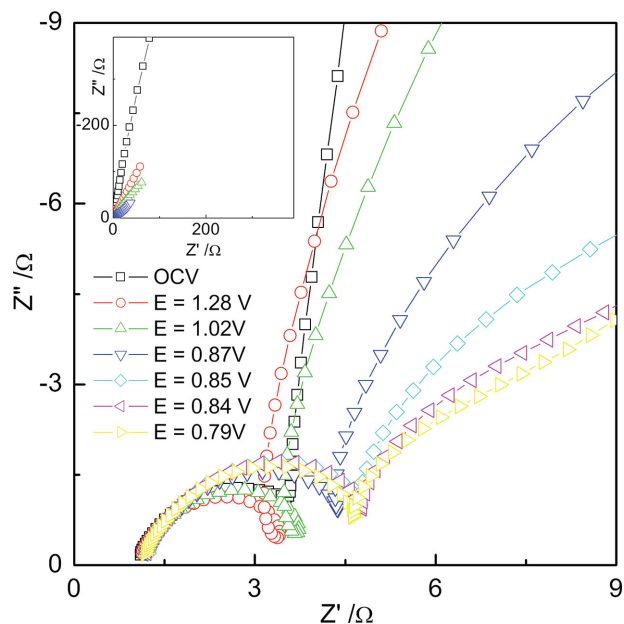

Figure 1. Open-circuit potential (E) vs. specific capacity (Q) of the ZFO-C vs. Li half-cell investigated during first Li uptake. Potential and capacity values are given for the points marked as (A), (B), (C), (D), corresponding to the samples investigated by XAS. (A) E = 2.53 V, Q = 0 mAh g^{-1}; (B) E = 1.02 V, Q = 83 mAh g^{-1}; (C) E = 0.87 V, Q = 167 mAh g^{-1}; (D) E = 0.79 V, Q = 417 mAh g^{-1}.

www.MaterialsViews.com

www.advenergymat.de

ADVANCED
ENERGY
MATERIALS

COMMUNICATION

subsequent cycles evidence stable reversible capacity values above 1000 mAh g^{-1} and efficiency values close to 100%. Based on this preliminary electrochemical results about SEI evolution, samples for ex situ XAS analysis have been prepared by submitting ZFO-C electrodes to selected Li uptakes via GITT, down to Li contents corresponding to points (A), (B), (C), (D) in Figure 1. GITT experiments have been performed in the aforementioned experimental conditions, in order to reproduce the several steps of SEI formation process. In particular, five samples were used in the subsequent set of XAS experiments: the fresh ZFO-C electrode (A); three electrodes corresponding to intermediate capacity stored during the first Li uptakes (B–D); the ZFO-C electrode resulting after a series of 20 charge/discharge cycles (hereafter indicated as E). The last sample (E) is intended as representative of a full developed SEI onto the electrodes. In fact, the full electrochemical characterization[13] of ZFO-C shows stable capacity values, i.e., 100% coulombic efficiency, after 20 cycles.

Soft XAS experiments were performed in a wide photon energy range (≈50–1100 eV) at the BL8.1L BEAR end-station of the ELETTRA synchrotron facility in Trieste (Italy).[14] The spectral energy was calibrated by referring to C 1s-π^* transitions. The incident light was horizontally polarized (mainly s-type) and the incidence angle of the light (with respect to the sample surface plane) was kept fixed at 10°. All XAS spectra were collected in total electron yield (TEY) mode (i.e., drain current mode) up to the carbon K-edge (≈286 eV) while at higher photon energies the photon emission signal (total fluorescence yield, TFY) was also collected. The incident photon flux was recorded for background subtraction and normalization using the photocurrent from the refocusing mirror. No evidence for X-ray damage of the electrodes was observed during the measurements. Sample status and transfers were strictly controlled at each stage of experiment, keeping the electrodes under inert atmosphere. In particular, argon atmosphere was used in a slightly overpressured glove-box where the samples were stored, in a transport-box (vacuum closed in a plastic bag) and in glove-bag, which was used to mount the samples in the BEAR chamber.

Chemical modifications occurring during the formation of the SEI can be monitored following the evolution of the absorption spectra of the relevant atomic species. Presence and oxidation of Li during the charging process are clearly seen looking at the Li K-edge data shown in **Figure 3**, left panel. During this process, Li$^+$ ions are buried inside the electrodes and partially contribute to the SEI formation. Due to the relatively low photon energy, only TEY spectra with typical 1 nm mean probing depth (MPD) can be collected so we cannot observe directly Li intercalation in the metal particles. As shown in Figure 3, the buildup of the SEI proceeds quite rapidly during the charging process, and the Li K-edge XAS signal clearly increase its intensity with
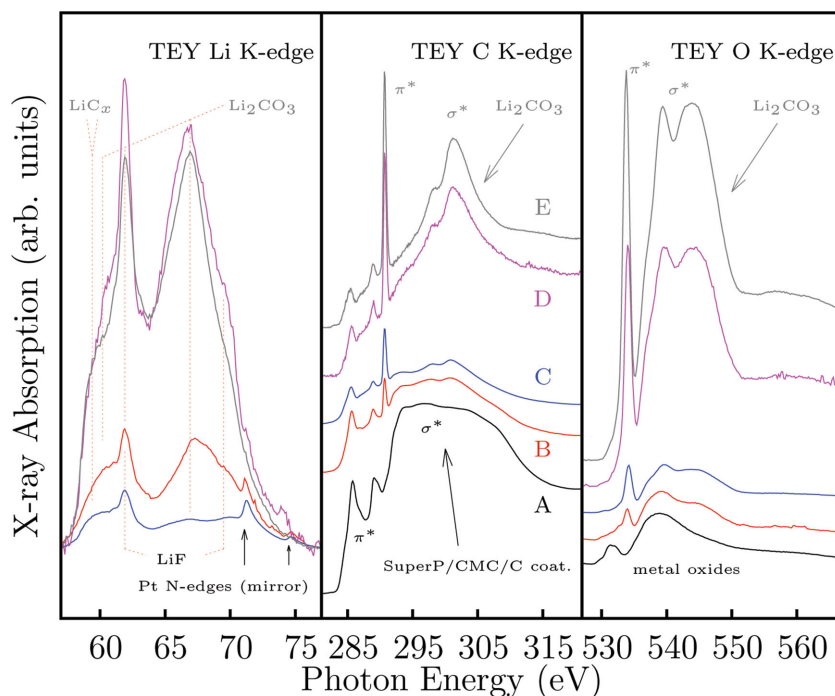

Figure 3. Li (left), C (center), and O (right-hand) K-edge XAS spectra collected using total electron yield (TEY) detection for the electrodes under consideration (A,B,C,D,E, see text and previous figures). The evolution of the XAS spectra reflects the formation of the SEI containing various chemical components as described in the figure and in the text.

the charge (see K-edge spectra for samples D and E). As mentioned above, the TEY signal shown in Figure 3 is related to the SEI region, due to the limited escape depths of the electrons. The main components of the Li K-edge TEY spectra are due to the presence[15–17] of LiF, Li$_2$CO$_3$ and LiC$_x$ in the SEI, as shown in Figure 3. These findings are in good agreement with previous models and determination of the SEI composition[2,18,19] at anode/electrolyte interface.

The evolution of the carbon and oxygen K-edge spectra confirms the increasing presence of Li$_2$CO$_3$ as shown in Figure 3 (center and right-hand panels). Strong features associated with the σ^* and π^* resonances are observed for higher charge values (sample D) and well-developed SEI (sample E). The C and O K-edge spectra for the fresh ZFO-C electrode (A) are compatible with the typical composition of the samples without the SEI. Carbon atoms in fresh electrodes are present into conductive SuperP, binder (CMC), and C-coating of the ZFO nanoparticles. The O K-edge TEY spectrum of the fresh electrode is compatible with that of metal oxides. For intermediate levels of charge (samples B and C), the spectra are a combination of components related to the SEI and to the fresh electrode.

The thickness evolution of the SEI can be monitored looking at the fading of the Zn and Fe signal of the ZFO nanoparticles being covered by the SEI layer, as discussed below. On the other hand, the formation of the SEI can be also studied looking at the intensity trend of the Na K-edge XAS spectra, which is initially present only in the CMC (nonactive) binder of the electrodes. As shown in **Figure 4** (left) the attenuation of the Na K-edge is quite important during the first Li uptake (B) but the signal is almost constant for higher levels of charge. The shape
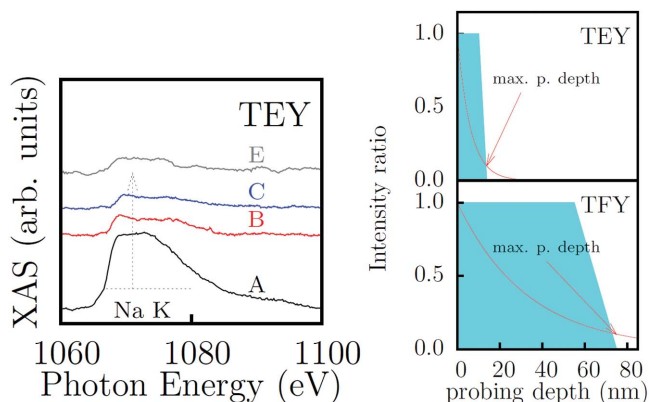
**ADVANCED
ENERGY
MATERIALS**

www.advenergymat.de

*Materials
Views*

www.MaterialsViews.com

Figure 4. Left panel: Na K-edge X-ray absorption (XAS) spectra collected using total electron yield (TEY) for the electrodes obtained during the first Li uptake (A–E, see text). The intensity trend is associated with the formation of the SEI. Right-hand panel: estimate of the different TEY and total fluorescence yield (TFY) probing depths (see text).

of the Na K-edge spectra is only slightly modified for increasing Li uptakes, indicating that Na atoms are modestly involved by chemical reactions and are still related to the CMC binder. As a matter of fact, the Na K-edge signal can be collected with the TEY technique indicating that the maximal average SEI thickness shadowing the signal of Na atoms is in the 10 nm range. This is not what happens for the TEY signals related to Fe and Zn (see **Figure 5**), that cannot be measured using this technique when the SEI is thicker (samples C,D,E). For those samples, XAS signals were collected using the TFY technique, which is more bulk sensitive.
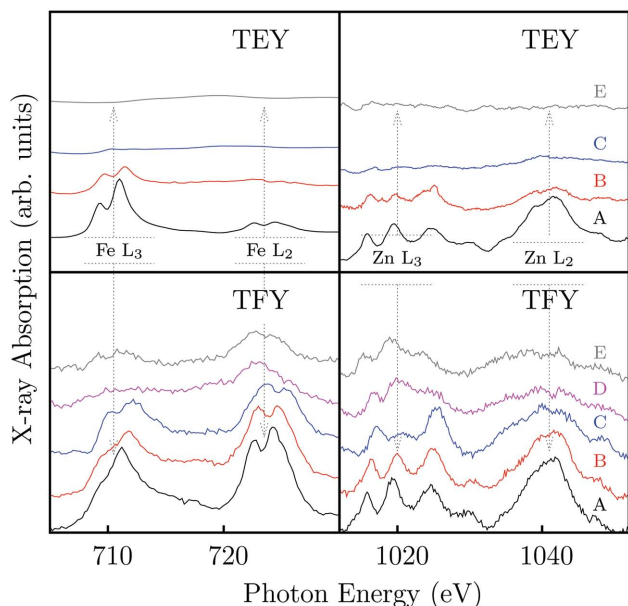
In fact, the MPD of soft X-ray absorption measurements (typical photon energies below 2 keV) in total electron yield (TEY) mode is known to be short,[10,12] being typically in the 2–10 nm range. On the other hand, fluorescence yield (TFY) MPDs are typically much longer, due to the weaker interactions of emitted photons with respect to the electrons. The two techniques appear thus to be largely complementary and able to provide a unique insight about the thickness of the interfaces created upon the X-ray absorbing materials. For the present active material of the electrodes ($ZnFe_2O_4$), it is thus useful to consider the intensity change of the relevant Fe and Zn photoabsorption signals during the formation of the SEI. A simple exponential law $I(d) = I_0 e^{-d/\lambda}MPD$ can mimic the intensity change of a selected photoabsorption signal as a function of the SEI thickness d, for a given mean probing depth λ_{MPD}. The TEY signal contains contributions from primary, Auger, and secondary electrons, so its probing depth is known to be dependent on the material and the core level energy under consideration.[12] We have found that the Auger electron effective range AER[12] is a good approximation for the MPD related to a porous material made up mostly of light elements, like the SEI formed at the surface of the electrodes. The AER increases almost linearly from 2 to 9 nm in the 70–1000 eV energy range. In Figure 4, top-right panel, we report a typical intensity trend for the TEY technique for soft X-ray measurements around 700 eV ($\lambda_{MPD}^{TEY} = 6$ nm), showing the useful probing depths (shaded). In the lower-right panel of Figure 4, we also report the useful probing depths for the TFY measurements around 700 eV ($\lambda_{MPD}^{TEY} = 30$ nm), evaluated by comparing the intensity of the XAS spectra of the two techniques. Those values are in good agreement with previous estimates of the probing depths of the two techniques.

The normalized XAS spectra associated with both the Fe L_2, L_3, and Zn L_2 and L_3 edges are shown in Figure 5, left and center panels respectively. Absorption signals were normalized to the incoming photon flux I_0. The intensity of the Fe L_2, L_3, and Zn L_2 and L_3 TEY signals (upper panels) is found to be strongly reduced already during the first Li uptake, and the absorption signals can be reliably measured only for samples A, B, and C. On the other hand, the intensity reduction for the TFY is found to be much less pronounced and the measurements were possible for all samples.

The intensity of the Fe, Zn, TEY photoabsorption spectra were found to follow quite closely an exponential attenuation trend. The thickness of the SEI interface at different charging steps was evaluated by combining the evolution of the intensity of both TEY and TFY XAS signals related to the Fe L_2, L_3, and Zn L_2 and L_3 core levels. The results are shown in **Figure 6**, in which the various thicknesses estimate for each sample and each absorption edge are presented. Results at different edges obtained by TEY data are shown in red (thickness below ≈ 15 nm) while those related to TFY are shown as blue points (thickness above 15 nm). The thick line for the estimated thickness is a guide for the eye and shows that a full SEI is already formed in sample D. These results are in good agreement with previous experimental findings typically indicating the thickness of the SEI formed at electrolyte/carbonaceous anode interfaces (as it is the case for ZFO-C) to be of the order of few tens of nanometers.[6,18,19] In Figure 6, we also show the estimated SEI thickness related to the Na K-edge intensity

Figure 5. Left panel: total electron (TEY, top) and fluorescence (TFY, bottom) yield XAS spectra at Fe (left) and Zn (right-hand) L-edges for the ZFO-C electrodes under consideration (A–E, see text and previous figures). The intensity trends reflect the evolution of the SEI upon the electrodes.
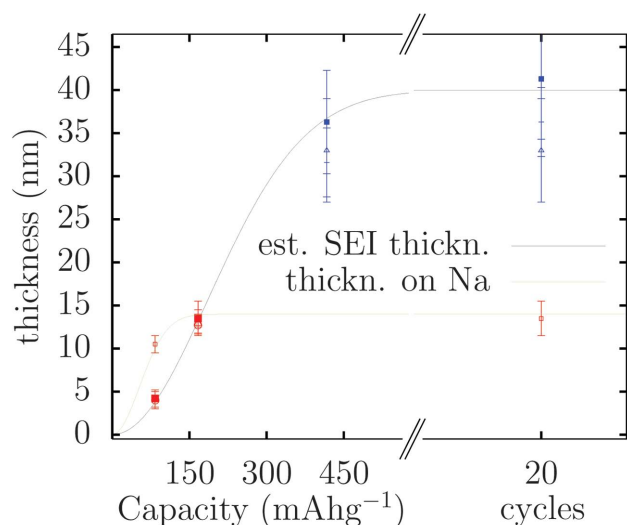
COMMUNICATION

Figure 6. SEI thickness as a function of capacity during first Li uptake and after 20 full charge/discharge cycles, as estimated by XAS intensity decay. Thickness values are evaluated both by TEY (red) and TFY (blue) XAS intensity trends at the Fe, Zn (L-edges), and Na K-edges. The estimated SEI thickness as detected by atoms included in the ZFO nanoparticles (Zn, Fe) grows up to about 40 nm, while that related to Na atoms (CMC binder) is limited to about 15 nm (lines are guide for the eye).

trend (see Figure 4). The XAS signal in this case is associated with the binder material of the electrodes. The trend shows that initially the SEI is formed on the whole binder+active particles system, but already at a specific capacity $Q = 417$ mAh g^{-1} (D), the SEI coverage is preferentially increased around the active particles. Present findings can be summarized in the model for SEI thickness increase in ZFO illustrated in **Figure 7** (bottom). A SEI thin layer is formed by percolation of the electrolyte inside the porous structure of the electrode, preferentially around the ZFO nanoparticles, in agreement also with previous findings for graphite electrodes (see ref.[6]). After a first stage of SEI formation covering binder and active nanoparticles, proceeding up to about 167 mAh g^{-1} (B), the SEI is accumulated preferentially around the ZFO nanoparticles. The different effective SEI thickness as detected from Na (binder) or Zn,Fe (ZFO nanoparticles) atoms results from this distribution inside the composite material forming the electrodes. Those results are consistent with the observation of the SEM image of the cycled ZFO-C electrode (Figure 7, top) which shows a different morphology as compared with that of uncoated ZFO (see SEM images in ref.[8]). Changes are associated with the SEI layer growing on the two electrode-active materials. In particular, the SEM image in Figure 7 does not show a thick SEI layer growing all over the electrode when ZFO-C is concerned. The SEI is found to grow preferentially over the active ZFO-C particles, in agreement with present findings by XAS. The absence of a thick SEI layer covering the electrode allows the easy movement of Li$^+$ ions into the electrode pores facilitating the (de)lithiation process.

The main conclusions that can be drawn by this work can be thus summarized as follows: 1) the evolution of the SEI takes place already during the first steps of the charging process and its thickness reach about 40 nm at about 1/3 of the full capacity,
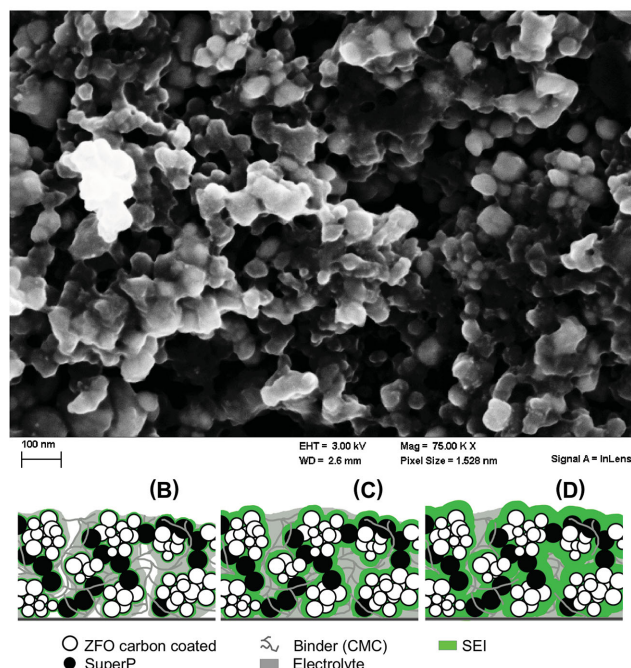

Figure 7. Bottom: Pictorial view of the SEI formation upon the ZFO-based electrodes under consideration. In an initial stage (left, sample B) a thin SEI is formed by electrolyte decomposition, while the electrolyte begins to percolate inside the porous electrode structure. In an intermediate phase during the Li uptake (center, sample C), the electrolyte is fully percolating inside the structure and the SEI grows around the active nanoparticles. At a later stage (right-hand, sample D), a thicker SEI is formed preferentially upon the ZFO nanoparticles. Top: The SEM image shows the surface of a cycled electrode (10 full charge/discharge cycles) evidencing the absence of the SEI on the electrode surface.

with a stable total thickness up to 20 working cycles; 2) the XAS technique is found to be very effective providing an estimate of the local thickness of the SEI, and indicates that the SEI grows preferentially around the ZFO nanoparticles.

Acknowledgements

[1] D. Aurbach, M. D. Levi, E. Levi, A. Schechter, *J. Phys. Chem. B* **1997**, *101*, 2195.
[2] E. Peled, *J. Electrochem. Soc.* **1998**, *145*, 3482.
[3] H. Buqa, A. Wursig, J. Vetter, M. E. Spahr, F. Krumeich, P. Novak, *J. Power Sources* **2006**, *153*, 385.
[4] S. Goriparti, E. Miele, F. De Angelis, E. Di Fabrizio, R. P. Zaccaria, C. Capiglia, *J. Power Sources* **2014**, *257*, 421.

**ADVANCED
ENERGY
MATERIALS**

www.advenergymat.de

**Materials
Views**

www.MaterialsViews.com

COMMUNICATION

[5] F. Martinez-Julian, A. Guerrero, M. Haro, J. Bisquert, D. Bresser, E. Paillard, S. Passerini, G. Garcia-Belmonte, *J. Phys. Chem. C* **2014**, *118*, 6069.

[6] P. Verma, P. Maire, P. Novk, *Electrochim. Acta* **2010**, *55*, 6332.

[7] D. Bresser, E. Paillard, R. Kloepsch, S. Krueger, M. Fiedler, R. Schmitz, D. Baither, M. Winter, S. Passerini, *Adv. Energy Mater.* **2013**, *3*, 513.

[8] F. Mueller, D. Bresser, E. Paillard, M. Winter, S. Passerini, *J. Power Sources* **2013**, *236*, 87.

[9] D. Bresser, F. Mueller, M. Fiedler, S. Krueger, R. Kloepsch, D. Baither, M. Winter, E. Paillard, S. Passerini, *Chem. Mater.* **2013**, *25*, 4977.

[10] M. Abbate, J. B. Goedkoop, F. M. F. de Groot, M. Grioni, J. C. Fuggle, S. Hofmann, H. Petersen, M. Sacchi, *Surf. Interface Anal.* **1992**, *18*, 65.

[11] M. Kasrai, W. Lennard, R. Brunner, G. Bancroft, J. Bardwell, K. Tan, *Appl. Surf. Sc.* **1996**, *99*, 303.

[12] B. H. Frazer, B. Gilbert, B. R. Sonderegger, G. D. Stasio, *Surf. Sci.* **2003**, *537*, 161.

[13] A. Varzi, D. Bresser, J. von Zamory, F. Mueller, S. Passerini, *Adv. Energy Mater* **2014**, *4*, 1400054.

[14] S. Nannarone, F. Borgatti, A. DeLuisa, B. P. Doyle, G. C. Gazzadi, A. Giglia, P. Finetti, N. Mahne, L. Pasquali, M. Pedio, G. Selvaggi, G. Naletto, M. G. Pelizzo, G. Tondello, *AIP Conf. Proc.* **2004**, *705*, 450.

[15] J. Tsuji, H. Nakamatsu, T. Mukoyama, K. Kojima, S. Ikeda, K. Taniguchi, *X-Ray Spectrom.* **2002**, *31*, 319.

[16] A. Braun, H. Wang, J. Shim, S. S. Lee, E. J. Cairns, *J. Power Sources* **2007**, *170*, 173.

[17] R. Qiao, Y.-D. Chuang, S. Yan, W. Yang, *PLoS One* **2012**, *7*, e49182.

[18] E. Peled, D. Golodnitsky, G. Ardel, *J. Electrochem. Soc.* **1997**, *144*, L208.

[19] S. Malmgren, K. Ciosek, M. Hahlin, T. Gustafsson, M. Gorgoi, H. Rensmo, K. Edstrom, *Electrochim. Acta* **2013**, *97*, 23.